THE JOURNAL OF BIOLOGICAL CHEMISTRY VOL. 287, NO. 7, pp. 4492–4502, February 10, 2012

Stimulation of Unprimed Macrophages with Immune Complexes Triggers a Low Output of Nitric Oxide by Calcium-dependent Neuronal Nitric-oxide Synthase*[S]

Received for publication, October 19, 2011, and in revised form, December 15, 2011 Published, JBC Papers in Press, December 28, 2011, DOI 10.1074/jbc.M111.315598

Zhi Huang[‡§], FuKun W. Hoffmann[‡], Jeffrey D. Fay[‡], Ann C. Hashimoto[‡], Moti L. Chapagain[¶], Pakieli H. Kaufusi[¶], and Peter R. Hoffmann[‡1]

From the [‡]Department of Cell and Molecular Biology and [¶]Department of Tropical Medicine, Medical Microbiology and Pharmacology, John A. Burns School of Medicine, University of Hawaii, Honolulu, Hawaii 96813 and the [§]Department of Biotechnology, College of Life Science and Technology, Jinan University, Guangzhou 510632, China

Background: Nitric oxide production by macrophages is conventionally attributed to inducible nitric-oxide synthase activity.
Results: Low levels of nitric oxide are generated by neuronal nitric-oxide synthase during engagement of Fcγ-receptors on unprimed macrophages.
Conclusion: Immune complexes trigger low output nitric oxide that promotes autocrine/paracrine phagocytosis.
Significance: A new role is identified for neuronal nitric-oxide synthase in macrophages.

Immune complexes composed of IgG-opsonized pathogens, particles, or proteins are phagocytosed by macrophages through Fcγ receptors (FcγRs). Macrophages primed with IFNγ or other pro-inflammatory mediators respond to FcγR engagement by secreting high levels of cytokines and nitric oxide (NO). We found that unprimed macrophages produced lower levels of NO, which required efficient calcium (Ca^{2+}) flux as demonstrated by using macrophages lacking selenoprotein K, which is required for FcγR-induced Ca^{2+} flux. Thus, we further investigated the signaling pathways involved in low output NO and its functional significance. Evaluation of inducible, endothelial, and neuronal nitric-oxide synthases (iNOS, eNOS, and nNOS) revealed that FcγR stimulation in unprimed macrophages caused a marked Ca^{2+}-dependent increase in both total and phosphorylated nNOS and slightly elevated levels of phosphorylated eNOS. Also activated were three MAP kinases, ERK, JNK, and p38, of which ERK activation was highly dependent on Ca^{2+} flux. Inhibition of ERK reduced both nNOS activation and NO secretion. Finally, Transwell experiments showed that FcγR-induced NO functioned to increase the phagocytic capacity of other macrophages and required both NOS and ERK activity. The production of NO by macrophages is conventionally attributed to iNOS, but we have revealed an iNOS-independent receptor/enzyme system in unprimed macrophages that produces low output NO. Under these conditions, FcγR engagement relies on Ca^{2+}-dependent ERK phosphorylation, which in turn increases nNOS and, to a lesser extent, eNOS, both of which produce low levels of NO that function to promote phagocytosis.

Macrophages are professional phagocytes that play a crucial role in innate immune responses against pathogens. IgG-opsonized proteins and microbes are engulfed through the receptors for the Fc portion of IgG (FcγRs)[2] on the surface of macrophages and other phagocytes (1, 2). FcγRI is the high affinity receptor that binds monomeric IgG2a in mice and IgG1 and IgG3 in humans (3). FcγRII and FcγRIII are low affinity receptors that require a higher avidity present on multivalent immune complexes (ICs) to effectively promote phagocytosis. FcγRIV is found in mice (the human ortholog is CD16A) and binds to IgG2a and IgG2b with intermediate affinity (4). FcγRI, -III, and -IV signal through an ITAM-containing γ chain that is associated with the small cytoplasmic domain of the receptors (5). Tyrosine phosphorylation of the ITAM results in the recruitment of Src homology 2-contianing molecules and adaptor proteins that propagate signals through downstream effectors. An important early effector enzyme in this signaling cascade is phospholipase Cγ, which cleaves phosphatidylinositol 4,5-bisphosphate to produce messenger molecules inositol 1,4,5-trisphosphate and diacylglycerol, the former of which triggers a rise in cellular Ca^{2+} levels. Although the effect of FcγR stimulation in generating a rapid, efficient Ca^{2+} flux has been established, the downstream effects of this increased intracellular Ca^{2+} on signaling pathways and the generation of soluble mediators are unclear.

FcγR engagement on macrophage during phagocytosis of IgG-opsonized microbes results in the secretion of pro-inflammatory mediators, including nitric oxide (NO). Secretion of NO during FcγR engagement has conventionally been measured

* This work was supported, in whole or in part, by National Institutes of Health Grant R21AT004844 and R01AI089999. This work was also supported by the Fundamental Research Funds for the Central Universities and the National Natural Science Foundation (Grant 20975045) of China.
[S] This article contains supplemental Fig. S1.
[1] To whom correspondence should be addressed: University of Hawaii, John A. Burns School of Medicine, 651 Ilalo St., Honolulu, HI 96813. Tel.: 808-692-1510; Fax: 808-692-1968; E-mail: peterh@pbrc.hawaii.edu.

[2] The abbreviations used are: FcγR, Fcγ receptor; IC, immune complex; BAPTA, bis(2-aminophenoxy)ethane tetraacetic acid; BMDM, bone marrow-derived macrophage; carboxy-PTIO, 2-(4-carboxyphenyl)-4,5-dihydro-4,4,5,5-tetramethyl-1*H*-imidazolyl-1-oxy-3-oxide, monopotassium salt; eNOS, endothelial nitric-oxide synthase; iNOS, inducible nitric-oxide synthase; nNOS, neuronal nitric-oxide synthases; KO, knockout; SelK, selenoprotein K; STIM1, stromal interaction molecule 1; MES, 2-[*N*-morpholino]ethanesulfonic acid; ops., opsonized; PGE_2, prostaglandin E_2.

only when the macrophages are first primed with lipopolysaccharide (LPS) or cytokines such as IFNγ and/or TNFα (6–8). This results in high-output NO that can exert cytotoxic effects on a variety of pathogens, including bacteria, viruses, fungi, and parasites (9, 10). However, the generation of low output NO by macrophages is emerging as an important event in the initiation or modulation of inflammatory responses. At lower levels, secreted NO plays an important role as a secondary messenger and can influence a wide variety of physiological and pathophysiological processes (11). Some processes affected by macrophage-derived NO include vasodilation, neural transmission, osteoclast homeostasis, and stimulation of other immune cells for enhanced inflammatory responses (12–15).

The enzyme isoforms that generate NO include inducible, endothelial, and neuronal nitric-oxide synthase (iNOS, eNOS, and nNOS). NO production by macrophages has mainly been attributed to expression of iNOS, which is induced by a variety of inflammatory cytokines or bacterial products like LPS (10). The nomenclature for nNOS and eNOS is derived from their detection mainly in brain tissue and blood vessels, respectively (16–18). Information regarding roles for eNOS and nNOS during macrophage activation has been limited. Low expression of nNOS has been detected in activated macrophages within atherosclerotic plaques of apoE KO mice (19). RAW264.7 mouse macrophages were shown to constitutively express eNOS, and LPS stimulation increased its activity via increased intracellular Ca^{2+} levels (20). However, the signaling pathways linking receptor-induced Ca^{2+} flux in macrophages to NO production and biological roles for NO remain unclear.

Our laboratory recently identified selenoprotein K (SelK) as an endoplasmic reticulum membrane protein important for efficient Ca^{2+} flux during the activation of immune cells (21, 22). Macrophages from SelK KO mice were impaired in FcγR-mediated Ca^{2+} flux, which enables the use of these macrophages to delineate signaling and effector functions that depend on Ca^{2+} flux. Using this approach, we found that FcγR stimulation on macrophages led to production of Ca^{2+}-dependent cytokines and, surprisingly, low levels of NO. This NO production was independent of iNOS and, instead, involved the Ca^{2+}-dependent activation of nNOS and, to a lesser extent, eNOS. Furthermore, activation of these enzymes required the Ca^{2+}-dependent phosphorylation of ERK, and the NO generated through this pathway enhanced the phagocytic capacity of other macrophages in Transwell assays. Overall, these findings reveal a novel Ca^{2+}-dependent signaling pathway and enzyme system in macrophages that produces low levels of NO during phagocytosis through FcγRs.

EXPERIMENTAL PROCEDURES

Mice—Generation of SelK KO mice was previously described (21). Littermate C57BL/6J wild-type controls were generated from mice originally purchased from the Jackson Laboratory. All animal experimental protocols were approved by the University of Hawaii Institutional Animal Care and Use Committee.

Antibodies and Reagents—Antibodies purchased from Cell Signaling, Inc. included anti-phospho-ERK (197G2), anti-total ERK (137F5), anti-phospho-JNK (81E11), anti-total JNK (2C6), anti-phospho-p38 (rabbit polyclonal), anti-total p38 (rabbit polyclonal), anti-iNOS (rabbit polyclonal), anti-nNOS (rabbit polyclonal), anti-eNOS (rabbit polyclonal), and anti-phospho-eNOS (Ser-1177 clone, C9C3). Others included anti-phospho-nNOS (Ser-1417 polyclonal, Millipore) and anti-β-actin (AC-74, Sigma). Secondary antibodies were purchased from Li-Cor Technologies. Antibodies for flow cytometry included APC-anti-CD16/32 (Ebioscience) and phycoerythrin-anti-CD64 (Biolegend). Bis(2-aminophenoxy)ethane tetraacetic acid (BAPTA, final concentration of 20 μM) was purchased from Invitrogen. Inhibitors purchased from EMD Biosciences included those specific for iNOS (2-methyl-2-thiopseudourea, sulfate, final concentration of 20 μM), nNOS ((4*S*)-*N*-(4-amino-5-(aminoethyl)aminopentyl)-*N*′-nitroguanidine, final concentration of 1.0 μM), eNOS (L-N5-(1-iminoethyl)ornithine, dihydrochloride, L-NIO, 2HCl; final concentration of 2.0 μM), total NOS (N^{γ},N^{γ}-dimethyl-L-arginine or dihydrochloride, ADMA; final concentration of 100 μM), and ERK1/2 (InSolution™ PD 98059; final concentration of 5.0 μM), JNK (EMD 420119, final concentration of 10 μM), and p38 (EMD 506148, final concentration of 2.0 μM). The NO scavenger, carboxy-PTIO (potassium salt, CAS 148819-94-7, final concentration of 100 μM) was purchased from Cayman Chemical. NOS1 (nNOS), NOS2 (iNOS), and NOS3 (eNOS) siRNA (sc-36091, sc-36092, and sc-36094, respectively) were purchased from Santa Cruz Biotechnology. BMDMs were transfected with these siRNA using a Neon electroporator (Invitrogen). Cyclohexamide was purchased from Tocris Bioscience.

Preparation of BMDMs—Bone marrow was flushed from femurs and tibiae with Hanks' balanced salt solution using a syringe with a 25-gauge needle. Cells were release from clumps by drawing the suspension through a syringe with an 18-gauge needle, and cell suspensions were then passed through a 40-μm pore cell strainer (BD Falcon) to remove tissue debris. The cells were plated in DMEM containing 10% FCS, 1% penicillin/streptomycin/L-glutamine (Invitrogen), and 10% L929 conditioned media and used on day 6 of culture. Levels of FcγR on BMDM from WT and SelK KO mice were evaluated prior to experiments as previously described (21).

Construction of Immune Complexes—Two types of IC were constructed: low and high avidity IC. Low avidity IC (IgG-opsonized (ops.) BSA) were constructed by incubating 20 μg of BSA (Invitrogen) with 200 μg of anti-BSA (Upstate/Millipore) in 500 μl of PBS (4:1 molar ratio anti-BSA to BSA), as previously described (21). After 1-h incubation at room temperature, the low avidity ICs were stored at 4 °C until use. The high avidity ICs (IgG-ops BSA coated beads, IgG-ops. beads) were constructed using 1.0 μm of yellow-green fluorescent, carboxylate-modified microspheres (Molecular Probes/Invitrogen). Bovine serum albumin (BSA, Invitrogen) was dissolved in 50 mM MES buffer, pH 6.0. Two milliliters of this BSA solution was added to 0.5 ml of a 2% aqueous suspension of the carboxylate-modified microspheres, and the mixture was incubated for 15 min at room temperature. To cross-link the BSA onto the beads, 40 mg of 1-ethyl-3-(3-dimethylaminopropyl)carbodiimide was added and mixed by vortexing. The pH was adjusted to 6.5 with dilute NaOH and incubated at room temperature for 2 h. Glycine was added at a final concentration of 100 mM to quench the

reaction, and the mixture was incubated for another 30 min. The microspheres were centrifuged at 18,000 × *g* for 20 min to separate the BSA-coated microspheres from unreacted protein. The coated beads were washed three times using PBS and centrifugation, then resuspended in 5 ml of PBS. An aliquot of these beads was saved for use as control beads, while another aliquot was opsonized with IgG. For opsonization, 10 μg of anti-BSA was added to 2×10^9 BSA-coated beads in 100 μl of PBS and incubated for 2 h. These IgG-ops. beads were washed with PBS and centrifugation as above and counted by hemocytometer prior to use.

Stimulation with IC and Western Blots—BMDMs were plated in 6-well plates (2×10^6 cells/well) with 1 ml of complete media. For low avidity IC stimulation, 30 μl of ops. BSA were added to each well for varied time periods as described in each figure legend. High avidity ICs or control beads were added at a ratio of 100:1 (beads:cells). For MAPK experiments, BAPTA was added (20 μM) for 1 h prior to adding ICs. For other experiments, NOS or MAPK inhibitors were added 1 h prior to adding ICs at final concentrations listed for each above. Cell lysates were prepared as previously described (21), and 30 μg of total protein was loaded per well on a 10–20% Criterion polyacrylamide gel (Bio-Rad), transferred to low fluorescence PVDF, and incubated with blocking buffer (both from Li-Cor, Inc.). Primary antibodies were added at 1:1,000 final dilution. Secondary antibodies (Li-Cor) were added at 1:10,000 final dilution, fluorescent signals were detected, and densitometry was measured using a Li-Cor Odyssey infrared imaging system.

Real-time PCR and Flow Cytometry—Upon stimulation of BMDMs with IgG-ops. beads for increasing time, cell pellets were harvested and total RNA was extracted using an RNeasy kit (Qiagen). Synthesis of cDNA was carried out using a High Capacity cDNA Synthesis kit (ABI), and real-time PCR was performed with iQ SYBR-Green Supermix (Bio-Rad) on a LightCycler 480 II real-time PCR amplification and detection instrument (Roche Applied Biosystems). Primers used included nNOS fwd: cat cag gca ccc caa gtt, nNOS rev: cag cag cat gtt gga cac a; eNOS fwd: cca gtg ccc tgc ttc atc, eNOS rev: gca ggg caa gtt agg atc ag; hprt fwd: tcc tcc tca gac cgc ttt t; and hprt rev: cct ggt tca tca tcg cta atc. Cycling conditions included 45 cycles with a hybridization temperature of 55 °C. For detection of FcγRs (CD16, CD32, and CD64) 5×10^5 BMDMs were suspended in 100 μl of PBS with 2% FBS and Fc-Block (Ebioscience) added before staining with 0.5 μg of phycoerythrin-anti-CD64. Similar conditions were used for staining with 0.5 μg of phycoerythrin-anti-CD16/32, except no Fc-Block was added. Fluorescence was measured on a FACScaliber (BD Biosciences), and data were analyzed with FlowJo 8.7 software.

Measurement of Cytokines, Eicosinoids, and NO—BMDMs were plated and stimulated as described above for MAPK detection. For cytokines and eicosinoids, BMDMs were stimulated for 20 h, media were harvested and centrifuged, and supernatants were stored at −80 °C until analysis was performed. Cytokines in supernatants were measured using a Cytometric Bead Array kit (BD Biosciences) per manufacturer's instructions. Leukotriene B4 and PGE_2 were analyzed using ELISA kits from R&D Systems. For NO measurement, BMDMs were plated and stimulated similar to the above method, and supernatants were harvested and NO measured using a nitric oxide assay kit based on the Greiss reaction (Pierce/Thermo Scientific). In some experiments, BMDMs were pretreated with inhibitors at concentrations listed above prior to stimulation with ICs. NO was then measured in the supernatant at 20 h post stimulation. We also used a more sensitive fluorometric technique (Abcam ab65327) to detect the low NO output and found similar differences between WT and SelK KO BMDMs (supplemental Fig. S1). Therefore, the Greiss reaction was used throughout the study for nitrite concentration as a measure of NO.

Phagocytosis Assays—BMDMs were plated on 10–15 mm^2 glass coverslips in 24-well plates with 0.5×10^6 cells/well in 10% L929 conditioned medium. Carboxy-PTIO was added at a final concentration of 100 μM for 2 h prior to addition of IgG-ops. beads (100:1, beads:cells) for 1 h. BMDMs were washed with PBS, fixed with 4% Pefabloc A, and mounted in DAPI-containing media. For Transwell experiments, BMDMs were added to glass coverslips in bottom chambers, the same as above, and to upper chambers (0.5×10^6 cells) and covered in 1.0 and 0.3 ml of 10% L929 conditioned medium, respectively. BMDMs in upper chambers were treated with inhibitors (at concentrations listed above) for 1 h followed by IgG-ops. beads (100:1, beads:cells) for 20 h. To control for the effects of inhibitors diffusing to lower chambers, inhibitors were added without IgG-ops. beads. After 20 h, the upper chambers were removed, and IgG-ops. beads were added to BMDMs in the lower chambers (100:1, beads:cells). After 1 h, BMDMs on coverslips were washed, fixed with 4% Pefabloc A, and mounted on slides with DAPI-containing mounting media. Images were captured on a Zeiss Axiovert 200M attached to a Zeiss LSM 5 Pascal imaging system with a minimum of 400 cells included per condition. ImageJ software was used to calculate the corrected total cell fluorescence with corrections for background fluorescence.

Statistical Analyses—Comparison of means was carried out using an unpaired Student's *t* test using GraphPad Prism version 4.0. All comparisons were considered significant at $p < 0.05$.

RESULTS

Secretion of Specific Mediators Requires SelK and High Avidity ICs—SelK is required for Ca^{2+} flux during FcγR-mediated activation of macrophages (21), but the importance of this Ca^{2+} flux for macrophage effector functions is not clear. We used BMDMs from WT and SelK KO mice to evaluate FcγR-induced cytokine and eicosinoid secretion. To stimulate FcγRs, high avidity ICs were constructed consisting of 1.0 μm BSA-coated beads opsonized with anti-BSA IgG, and anti-BSA-ops. BSA (low avidity IC) and BSA-coated beads served as controls. IC-stimulated BMDMs were analyzed for secretion of PGE_2, leukotriene B4, IL-6, IL-10, IL-12, MCP-1, MIP-3α, TNFα, and IFNγ, only five of which were found at detectable levels: PGE_2, IL-6, TNFα, MCP-1, and MIP-3α (Fig. 1). Optimal secretion of PGE_2, IL-6, and TNFα required both SelK expression and high avidity ICs, with TNFα the most affected by SelK deficiency (50% decrease compared with WT). In contrast, MCP-1 and MIP-3α secretion required high avidity ICs, but not SelK expression, for optimal levels. Despite the fact that the BMDMs

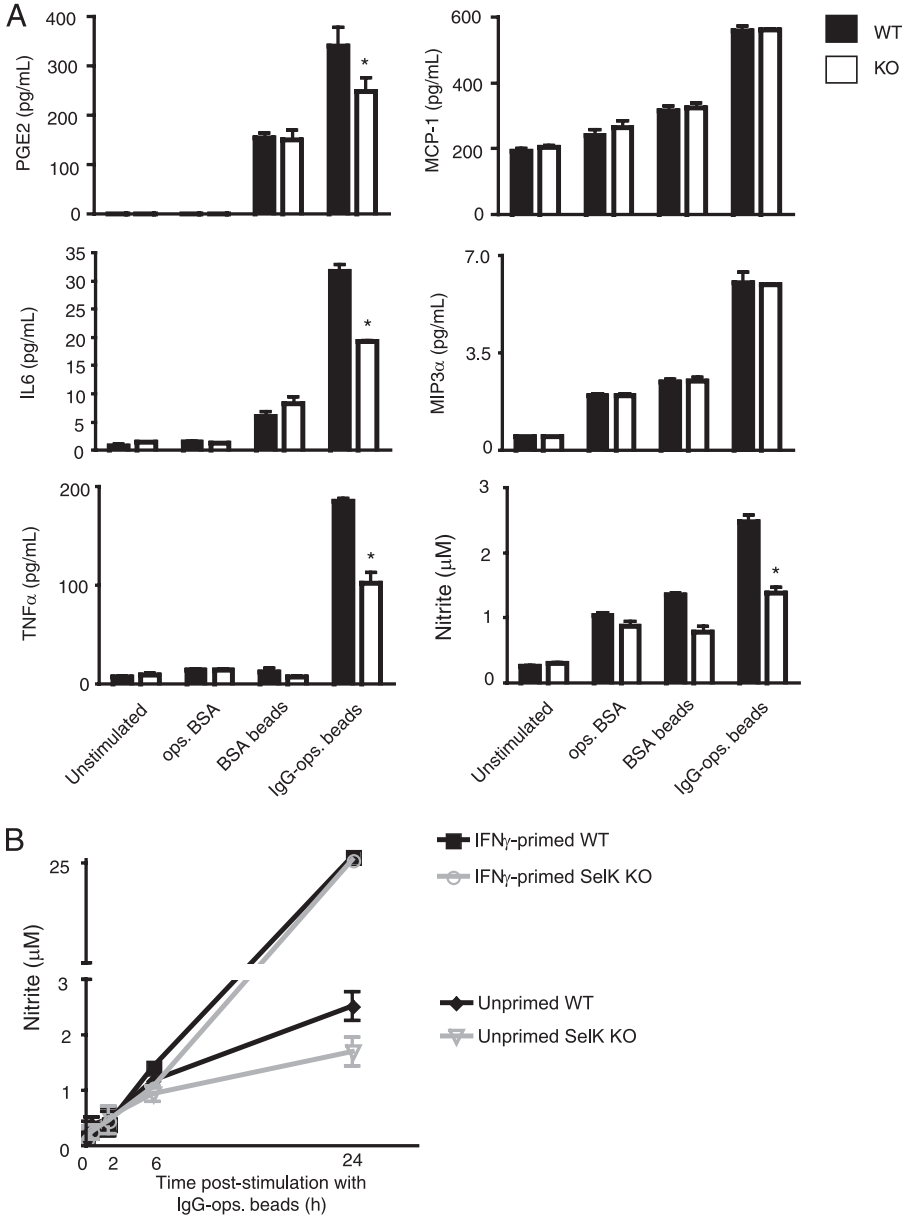

FIGURE 1. **Secretion of soluble mediators induced by FcγR stimulation.** *A*, BMDMs were stimulated for 20 h with low avidity IC (*ops. BSA*), control beads (*BSA beads*), and high avidity IC (*IgG-ops. beads*). Results are expressed as means ± S.E. ($n = 3$). *, $p < 0.05$ comparing SelK KO to WT within each treatment group. Results indicate that optimal secretion of PGE_2, IL-6, TNFα, and NO (as determined by nitrite concentration) required both SelK expression and high avidity ICs, whereas MCP-1 and MIP-3α only required high avidity ICs. *B*, WT or SelK KO BMDMs were or were not primed with IFNγ (200 pg/ml) for 36 h, then IgG-ops. beads were added for 0, 2, 6, or 24 h, and media were collected to measure nitrite levels as a measure of NO.

were not primed with inflammatory stimuli, FcγR stimulation produced NO. Similar to TNFα, levels of NO produced from SelK KO BMDM stimulated with high avidity ICs were decreased to 50% of WT controls. Interestingly, high output NO from IFNγ-primed BMDMs did not require SelK (Fig. 1*B*). Given that NO secretion from FcγR-stimulated macrophages has conventionally been attributed to iNOS in primed macrophages (6, 7, 13, 23), we further examined the signaling and functionality of low output NO production in unprimed BMDMs.

Low Output NO Is Generated by nNOS and Requires SelK—The levels of IC-stimulated NO produced by unprimed BMDMs were low relative to primed BMDMs, suggesting that FcγR stimulation did not result in high output NO through iNOS typical of primed BMDMs (24). Consistent with this notion, we found that iNOS expression was not induced through FcγR stimulation in unprimed BMDMs (Fig. 2*A*). However, both total and phosphorylated nNOS levels were increased with high avidity IC, and this effect was diminished by SelK deficiency (Fig. 2, *A* and *B*). To our knowledge, this is the first report of a receptor system that up-regulates nNOS expression in macrophages. Low levels of total eNOS were also detected and were unaffected by addition of high avidity IC, but phosphorylated eNOS was slightly increased with high avidity IC and required SelK. It also is worth noting that SelK expression was increased, particularly with high avidity IC. Stimulation of BMDMs with IgG-ops. beads increased nNOS mRNA (Fig. 2*C*), and the NO production induced by IgG-ops. beads

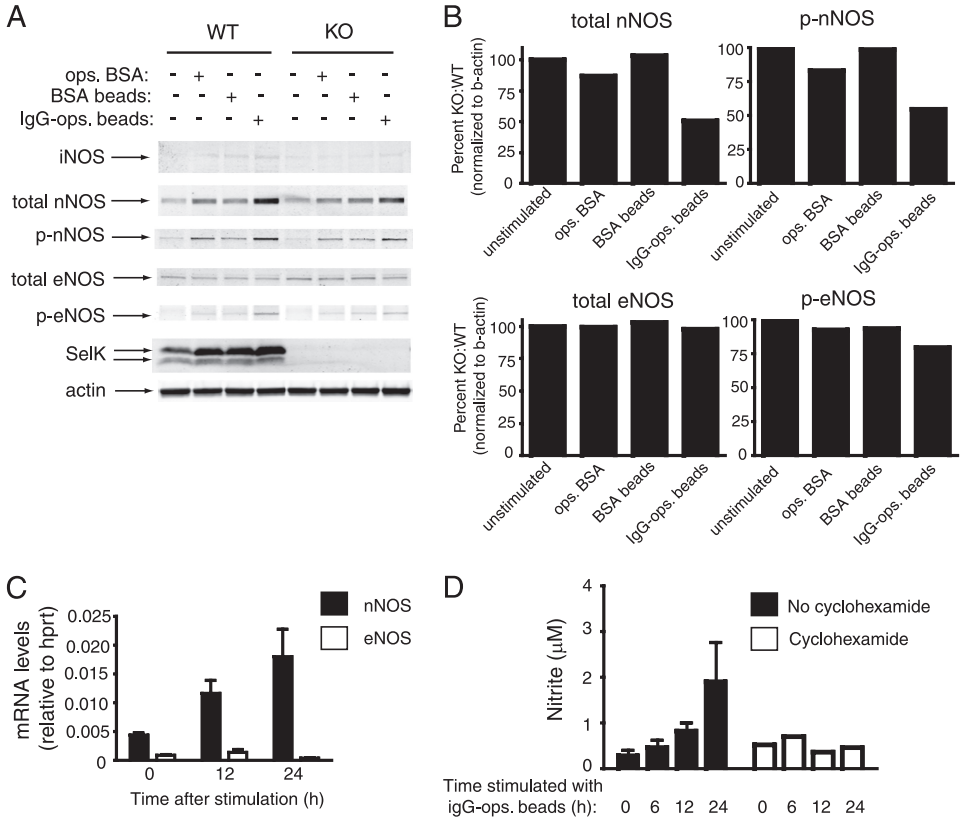

FIGURE 2. **Increased expression of nNOS is induced in macrophages by high avidity IC.** *A*, Western blot analysis of lysates from WT and SelK KO BMDMs were collected 20 h after addition of high avidity ICs composed of IgG-ops. beads, or osp. BSA, or BSA beads as controls. Results show IgG-ops. beads increased total and phosphorylated nNOS and, to a lesser extent, phosphorylated eNOS, and this was higher in WT compared with KO BMDMs. Expression of iNOS was not detected, and β-actin was used as a loading control. *B*, densitometry was performed on total and phosphorylated nNOS and eNOS comparing KO to WT. Results are representative of two independent experiments. *C*, real-time PCR was used to determine mRNA levels for nNOS and eNOS relative to the housekeeping mRNA, hypoxanthine-guanine phosphoribosyltransferase (*hprt*). *D*, IgG-ops. beads were added to BMDMs in the presence or absence of cyclohexamide (final concentration of 10 μM), and at different time points supernatants were collected for determining nitrate concentration as a measure of NO. Results for *C* and *D* are expressed as means ± S.E. ($n = 3$).

required new protein synthesis (Fig. 2*D*). These results suggest that FcγR stimulation increases nNOS gene transcription that leads to increased nNOS protein and activity.

To functionally characterize the role of the different NOS during FcγR stimulation of macrophages, we utilized inhibitors against each individual NOS as well as a total NOS inhibitor. Results demonstrated that inhibiting nNOS decreased NO production, whereas inhibiting eNOS and iNOS had slight and no effects, respectively (Fig. 3*A*). The decrease in NO caused by the nNOS inhibitor was not as strong as the effects of the total NOS inhibitor. This result, together with the small NO decrease caused by the eNOS inhibitor, suggests that eNOS contributes a small amount to the production of FcγR-induced NO, but nNOS is the major contributor. As an alternative method, we used siRNA to inhibit the expression of the different NOS isoforms and confirmed that nNOS siRNA had the most significant effect on NO production (Fig. 3, *B* and *C*). Overall, these data suggest that nNOS, and to a lesser extent eNOS, are important enzymes involved in secretion of low output NO during FcγR stimulation of macrophages.

FCγR Stimulation Activates ERK in a Ca^{2+}-dependent Manner—FcγR engagement has been shown to activate mitogen-activated protein kinase (MAPK) signaling in macrophages within 5–20 min, which leads to pro-inflammatory cytokine production (25, 26). However, little is known regarding the relationship between MAPKs and Ca^{2+} flux during NO production by macrophages. We first examined the effect of impaired Ca^{2+} flux on FcγR-mediated MAPK activation using both SelK-deficient BMDMs and WT BMDMs pretreated with the Ca^{2+}-chelating reagent, BAPTA. High avidity IC induced phosphorylation of all three MAPKs: ERK, JNK, and p38 (Fig. 4). Phosphorylation of both ERK and p38 peaked within 5 min of FcγR stimulation, and phosphorylation of JNK occurred at 15 min. Both SelK deficiency and BAPTA pretreatment decreased ERK phosphorylation to ~50% of WT controls, whereas phosphorylation of p38 and JNK were slightly affected or unaffected, respectively. Overall, these data suggest that p-ERK is more dependent on Ca^{2+} compared with p-JNK or p-p38 during FcγR engagement.

Activation of ERK Is Required for Activation of nNOS and NO Secretion—The data above suggested that optimal activation of ERK and nNOS was dependent on Ca^{2+} flux during FcγR stimulation, so we next used inhibitors to determine the relative importance of these molecules for NO secretion. BMDMs were pretreated with inhibitors for each MAPK (ERK, p38, and JNK) followed by addition of high avidity IC and measurement of NO. The ERK inhibitor significantly reduced FcγR-induced NO secretion, whereas p38 and JNK

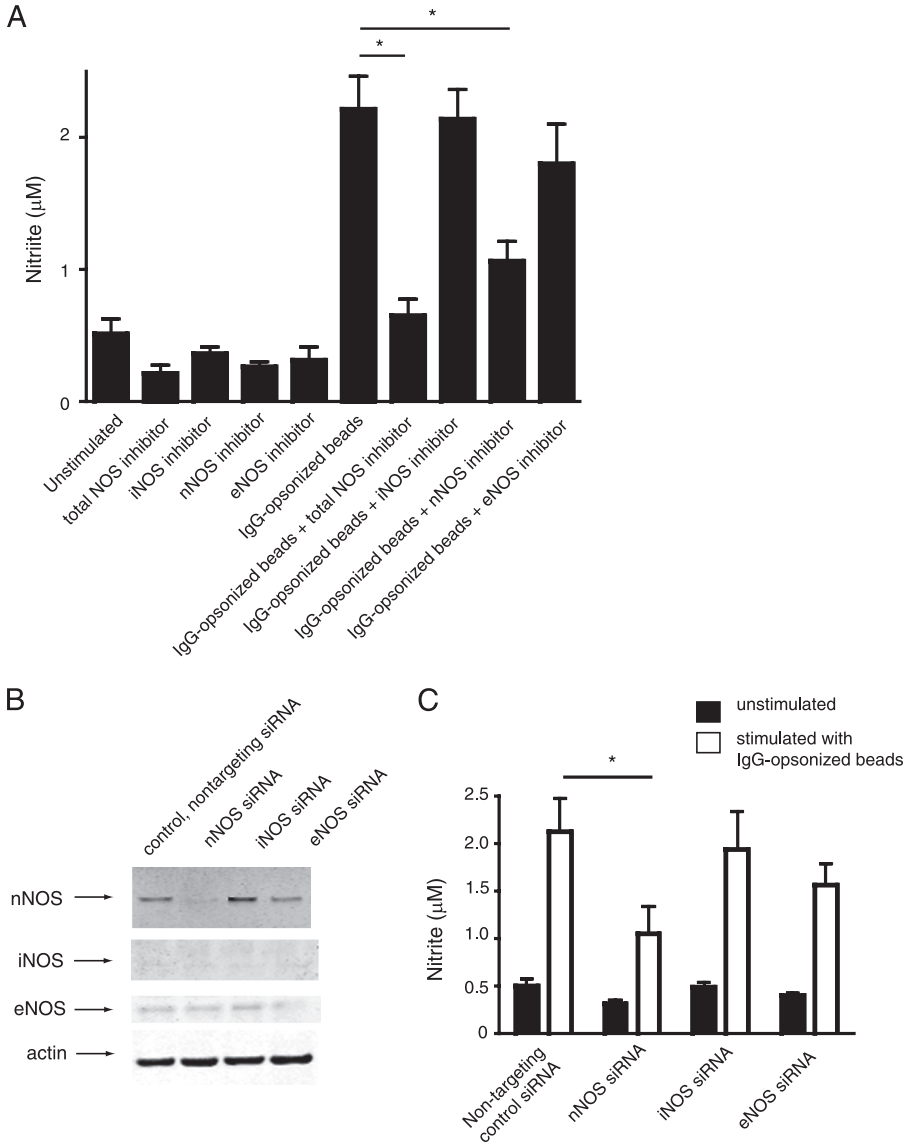

FIGURE 3. **FcγR-induced NO is predominantly produced by nNOS.** *A*, WT BMDMs pretreated with inhibitors against total NOS or individual NOS were or were not stimulated with IgG-ops. Beads, and secreted nitrate was measured as an indicator of NO levels. *B*, BMDMs were transfected with siRNA, and after 30 h the effects on expression of nNOS, iNOS, and eNOS were evaluated using Western blotting with β-actin as a loading control. *C*, the effects of nNOS, iNOS, and eNOS siRNA on nitrite as a measure of NO production 20 h after stimulation with IgG-ops. beads show reducing nNOS expression reduced NO production. Results are expressed as means ± S.E. ($n = 3$). *, $p < 0.05$.

inhibitors showed only a slight reduction and no effect, respectively (Fig. 5*A*).

Because ERK activation occurs rapidly after FcγR stimulation and full activation was Ca^{2+}-dependent in a manner similar to nNOS activation, we hypothesized that ERK activation was required for increased nNOS expression and/or phosphorylation. Using inhibitors specific for each MAPK, we evaluated relative levels of each NOS isoform by Western blot. Results indicated that FγcR-induced increases in total nNOS were reduced with inhibitors for each MAPK, but inhibition of ERK reduced phosphorylation of nNOS (Fig. 5*B*). Phosphorylation of eNOS was also slightly reduced with ERK inhibition. Similar to results above, iNOS expression remained very low regardless of MAPK inhibition. These data suggest that ERK, the MAPK most dependent on Ca^{2+} flux, is the major MAPK that contributes to both increased expression and phosphorylation of nNOS after FγcR stimulation in macrophages.

Phagocytosis of High Avidity ICs Is Impaired in Macrophages from SelK KO Mice—The low output of NO induced by FcγR stimulation on macrophages may reflect a role for this reactive species as a mediator as opposed to a cytotoxic compound for killing pathogens. Low levels of NO have been suggested to promote phagocytosis (27), so we performed phagocytosis assays in the absence and presence of the NO scavenger, carboxy-PTIO to show the autocrine/parocrine effects of FcγR-induced NO. Addition of the scavenging compound effectively reduced NO in the media and reduced the uptake of IgG-ops. beads (Fig. 6, *A* and *B*). To further investigate the role of NO synthases and ERK, we used a Transwell system to evaluate the paracrine effects of FcγR-induced NO on the phagocytic capacity of neighbor macrophages. BMDMs in the upper chambers were stimulated with high avidity ICs, allowing soluble mediators to diffuse into BMDMs in the lower chambers. These BMDMs in the lower chambers were then evaluated for their

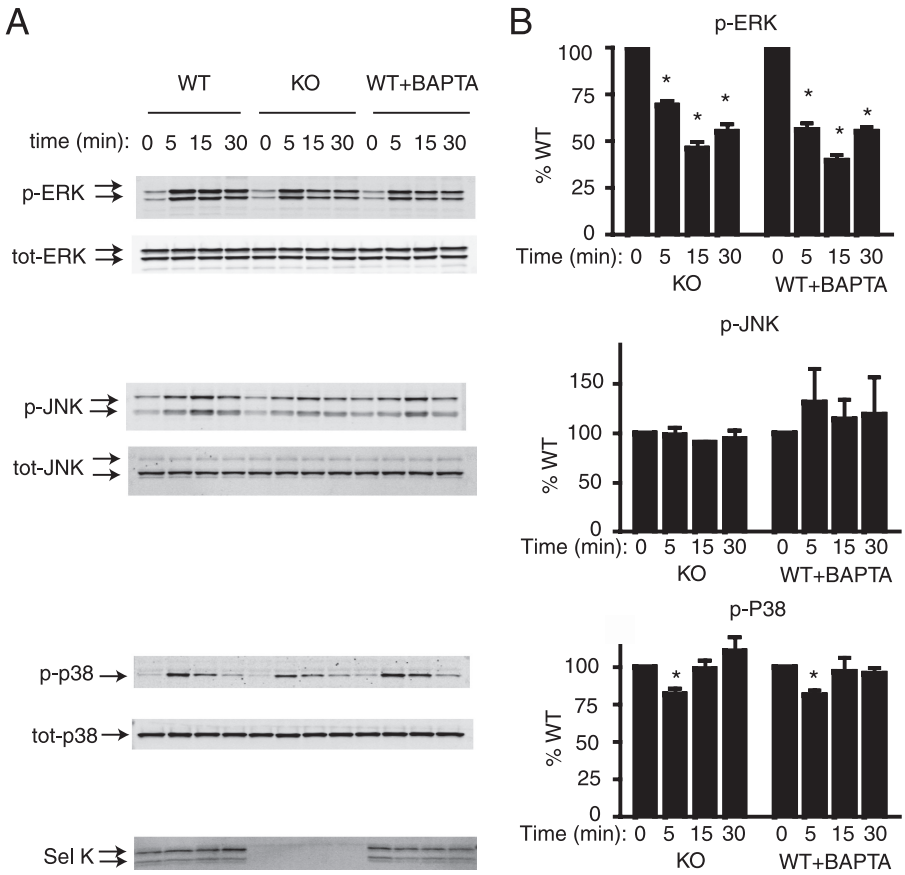

FIGURE 4. **MAPK activation induced in macrophages by high avidity IC.** *A*, IgG-ops. beads were added to BMDMs, and cells were lysed after each time point as indicated. Western blot analyses of lysates included antibodies against phosphorylated and total ERK, JNK, and p38, as well as anti-SelK. WT cells were pretreated with BAPTA as a Ca^{2+}-chelator to determine the dependence of each MAPK on Ca^{2+} flux for activation. *B*, densitometry was performed on blots from three experiments for levels of p-ERK/total ERK, p-JNK/total JNK, and p-p38/total p38, and percentages for SelK KO compared with WT were graphed for each. Results are expressed as means ± S.E. *, $p < 0.05$.

phagocytic capacity, and results demonstrated that soluble mediators generated in the upper chambers significantly increased phagocytosis of IgG-ops. beads by BMDMs in the lower chambers (Fig. 6, *C* and *D*). To determine whether NO production was a major contributor to this increased phagocytic capacity, we pretreated the BMDMs in the upper chamber with the total NOS inhibitor prior to high avidity IC addition. This resulted in lower phagocytic capacity for BMDMs in the lower chamber compared with Transwells in which no inhibitor was included with IgG-ops. beads, confirming that FcγR-induced NO from BMDMs in the upper chamber contributed to increasing phagocytic capacity of BMDMs in the lower chamber. Using a similar approach with an ERK inhibitor, we found that ERK activation in BMDMs in the upper chamber was required for full phagocytic capacity of BMDMs in the lower chamber BMDMs. However, these inhibitors did not completely eliminate the pro-phagocytic effects of high avidity ICs, suggesting NOS or ERK only partially contributed to FcγR-induced mediator secretion, and this is consistent with our signaling data above. Overall, these results suggest FcγR stimulation on macrophages produces low output NO that functions to promote phagocytosis by neighbor macrophages.

DISCUSSION

The role of NO production by macrophages during the phagocytosis of IC has mainly been associated with the cytotoxic activity of these cells for killing ingested or attached microbes (9, 10). In fact, FcγR-mediated engulfment by macrophages has been consistently studied by first priming the macrophages with pro-inflammatory cytokines, which results in strong activation and secretion of high levels of NO. A central step in this high output NO process is the expression of iNOS, and indeed iNOS has become a reliable biomarker for fully activated macrophages (28). In the present study, we reveal a novel signaling pathway activated through FcγR stimulation of unprimed macrophages that leads to low output NO (Fig. 7). This NO production does not involve iNOS, but instead relies on nNOS and, to a lesser extent, eNOS. The NO levels produced during FcγR stimulation were low compared with those typically exhibited by iNOS in primed macrophages. However, this low output NO was functionally active as demonstrated by its ability to promote phagocytosis of ICs by neighboring macrophages. Thus, the NO generated by nNOS and eNOS during FcγR stimulation in unprimed macrophages is more likely to serve as a secondary messenger than as a cytotoxic molecule.

Both nNOS and eNOS are conventionally regarded as constitutively expressed enzymes found in several cell types, and both are thought to be involved in the basal regulation of cellular physiology and metabolism (29). The FcγR-mediated activation of nNOS and, to a lesser extent, eNOS in macrophages

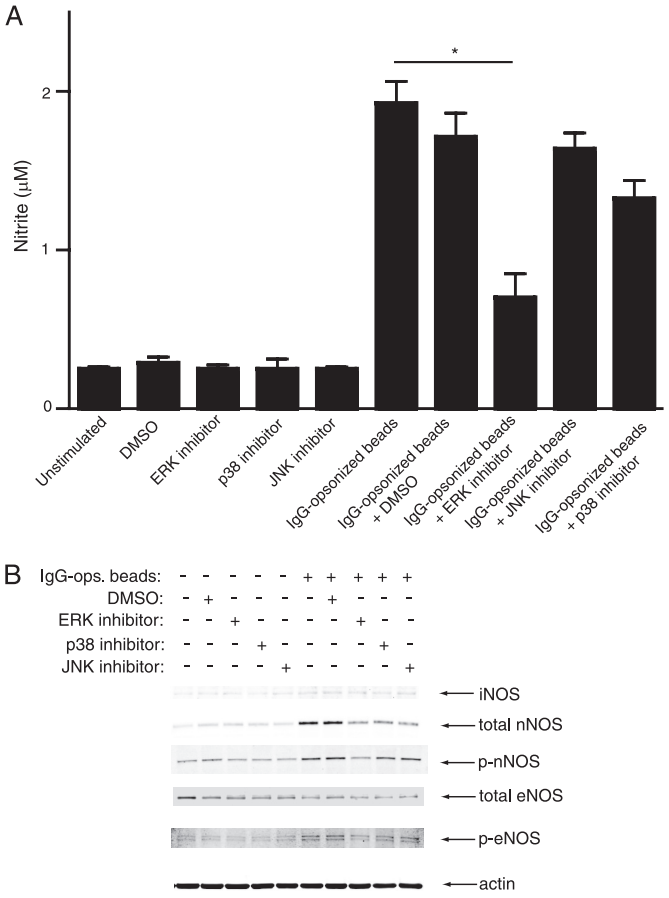

FIGURE 5. **Roles for different MAPKs in NO production.** *A*, as measured by nitrite, NO was released by WT BMDMs after stimulation with high IgG-ops. beads for 20 h, and pretreatment with inhibitors against individual MAPKs show a significant decrease with ERK inhibition. Results are expressed as means ± S.E. ($n = 3$). *, $p < 0.05$. *B*, Western blot analysis of lysates from WT BMDMs demonstrating the effects of individual MAPK inhibitors on levels of iNOS or total/phosphorylated nNOS and eNOS. β-Actin was used as a loading control.

demonstrated in the present study represents a new role for these NOS isoforms in inflammation and immune responses. The lack of detection of nNOS and eNOS expression in other studies involving stimulated macrophages likely is due to the fact that high output NO may actually inhibit expression and activity of these NOS isoforms (30, 31). In fact, an iNOS-deficient clone derived from RAW 264.7 murine macrophages, called CRL-2278, exhibited nNOS activity in response to LPS or IFNγ (32). This study, together with our data, suggests that nNOS activity that may occur *in vivo* under conditions in activated macrophages can be detected only under conditions in which iNOS is not expressed.

The nomenclature of nNOS and eNOS is derived from their detection in brain tissue and blood vessels, respectively (16–18). However, our data demonstrate that nNOS expression is actually increased in FcγR-stimulated macrophages, suggesting its expression may be more inducible than constitutive in these cells. Consistent with this notion, low expression of nNOS has been detected in activated macrophages within atherosclerotic plaques of apoE KO mice (19). Similarly, eNOS expression has not been widely described in macrophages, but eNOS in BMDMs was shown to constitutively generate low levels of NO that acted to positively enhance iNOS expression upon LPS stimulation (12). Our findings demonstrated that total eNOS levels were not affected by FcγR stimulation in macrophages, but activated eNOS was slightly increased. Thus, our data open a new line of investigation regarding the expression and/or activation of these two NOS isoforms in generating low output NO for the initiation or modulation of immune responses.

Our finding, that nNOS and eNOS activation are dependent on Ca^{2+} flux, is consistent with earlier findings showing the presence of Ca^{2+}-dependent, NO production at low levels. For example, Ca^{2+}-dependent NOS activity was detected in membrane extracts from unstimulated J774.1 murine macrophages (33). Also, the human monocytic U937 cell line expresses eNOS, and its activity is Ca^{2+}-dependent (34). In contrast, production of NO by iNOS has been shown to be independent of Ca^{2+} flux (13, 23), and our data support the notion that Ca^{2+}-dependent signaling during FcγR stimulation in macrophages does not involve this NOS isoform. The findings in this current study demonstrate that optimal FcγR-induced effector functions in macrophages depend on SelK expression, although the knockout of SelK in the macrophages did not totally eliminate FcγR-induced signaling or effector function. As shown in Figs. 1 and 2, and SelK deficiency resulted in ~50% reduction in TNFα and NO secretion compared with WT controls. Consistent with these effects, SelK deficiency also decreased ERK activation by 50%. The facts that BAPTA pretreatment had the same effects on ERK activation and that we previously demonstrated a requirement for SelK for FcγR-induced Ca^{2+} flux in macrophages support the use of SelK-deficient macrophages for identifying Ca^{2+}-dependent signaling pathways. However, it is important to note that the FcγR-induced effects are only partially dependent on SelK and Ca^{2+} flux. In this sense, Ca^{2+} flux likely functions to activate signaling molecules (mainly ERK and slightly p38), but Ca^{2+}-independent signals (like JNK and others) generated during FcγR-induced phagocytosis are also important for effector functions.

The Transwell experiments presented in this study demonstrate that the NO generated by BMDMs during FcγR stimulation functions in a paracrine manner to promote phagocytosis of high avidity ICs by neighbor BMDMs. We did not observe increased FcγR expression on the BMDMs in the lower chamber (data not shown), and we are currently investigating the mechanisms by which low output NO increases phagocytic capacity. NO has been estimated to diffuse quickly from its source and is therefore believed to only act in close proximity to the cells producing it (35, 36). However, our data showed diffusion of functional NO to the BMDMs in the lower chamber, which represents a relatively long distance to reach the target cell population. This suggests that the diffusible range for NO may actually be quite larger than previously believed. Inhibitors of both NOS and ERK decreased the paracrine effects of FcγR-induced NO on phagocytosis of BMDMs in the lower chamber, indicating that NO production by the BMDMs in the upper chamber was important and required ERK activation. However, we cannot rule out autocrine effects occurring in the lower chamber that may have enhanced secretion of mediators as well. NO has been shown to promote phagocytosis in other studies, although the NO measured in these experiments were

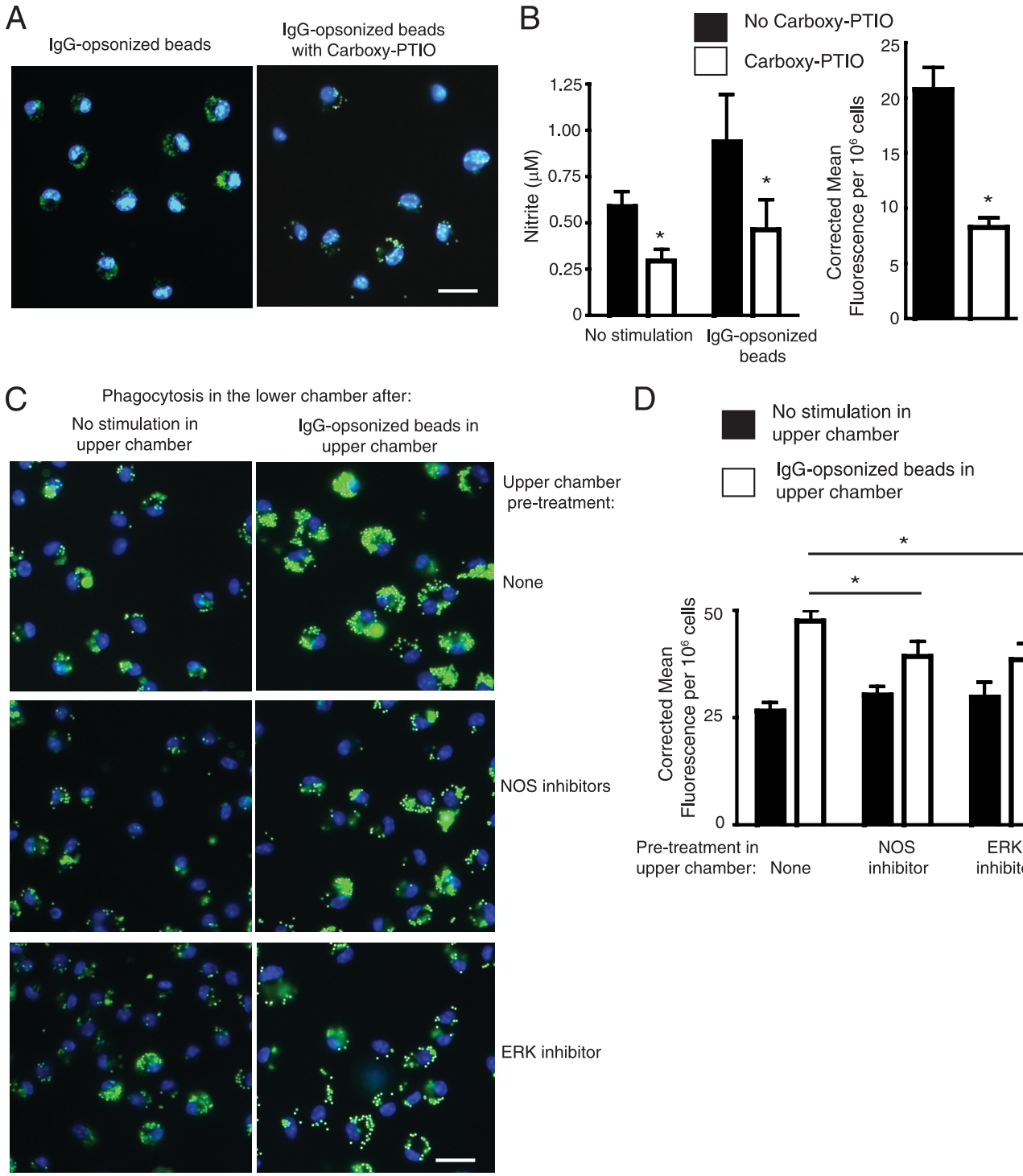

FIGURE 6. **NO produced during FcγR-mediated engulfment increases phagocytosis of neighbor macrophages.** *A*, representative images of experiments in which IgG-ops. beads were added to WT BMDMs in the absence or presence of the NO scavenger, carboxy-PTIO. *B*, NO levels as determined by nitrite measurement in the media after 20-h incubation with the IgG-ops. beads showed decreased NO with carboxy-PTIO included in the media. Also, phagocytosis was quantified by measuring corrected total cell fluorescence per 10^6 cells and was decreased when carboxy-PTIO was included in the media. *C* and *D*, Transwell assays were performed with BMDMs in the upper chambers pretreated with no inhibitor or with NOS or ERK inhibitors for 1 h prior to no stimulation (*left panels*) or stimulation with IgG-ops. beads (*right panels*). After 20 h, the top chambers were removed and IgG-ops. beads were added to BMDMs in the lower chambers, and phagocytic capacity was determined by fluorescence microscopy. Representative images of BMDMs in the lower chambers are shown in *C*, where BMDMs in the upper chambers were pretreated with no reagent or total NOS inhibitor or ERK inhibitor, followed by stimulation with high avidity ICs, or after pretreatment with either total NOS inhibitor or ERK inhibitor. Phagocytosis was quantified by measuring corrected total cell fluorescence per 10^6 cells. To control for potential diffusion of inhibitors into bottom well, inhibitors were added in the absence of IgG-ops. beads, and no effects were found when NOS or ERK inhibitors were added into the top chambers compared with unstimulated BMDMs in the upper chamber, indicating no detectable diffusion of inhibitors into bottom chambers. For *A* and *C*, nuclei were stained with DAPI, whereas internalized fluorescent beads appear *green*. *Scale bar* represents 25 μm. For *B* and *D*, results are expressed as means ± S.E. ($n = 3$). *, $p < 0.05$.

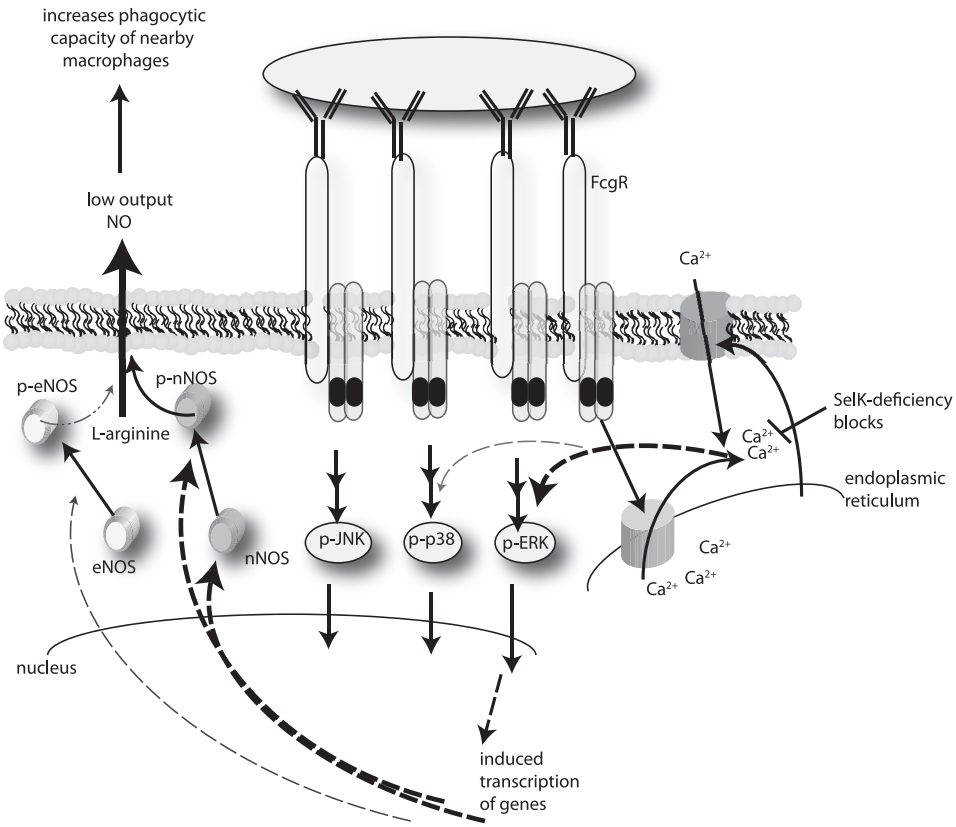

FIGURE 7. **Model for FcγR-mediated secretion of low output NO by macrophages.** Engagement of FcγR on the surface of macrophages induces rapid store-operated Ca^{2+} entry, which leads to marked increases in total ERK and phosphorylation of ERK, and small increases in phosphorylation of p38. These factors together with Ca^{2+}-independent JNK activation regulate gene transcription. In particular, pERK up-regulates expression of nNOS and factors that increase phosphorylation of nNOS and slightly increase phosphorylation of eNOS. Increases in activity of nNOS and, to a lesser extent, eNOS lead to low output NO that functions to increase phagocytic capacity of neighbor macrophages.

iNOS-derived (27, 37). Our study is the first to show that nNOS is a major contributor to pro-phagocytic NO. In support of the importance of nNOS is the fact that *Bacillus anthracis* has evolved to generate a lethal factor (LeTx) that specifically cleaves nNOS in macrophages and does not cleave either iNOS or eNOS (38).

The requirement of effective Ca^{2+} flux in macrophages during phagocytosis and effector functions has been established (39–41), although the role of Ca^{2+} for the specific steps of these processes is not entirely clear. The role on Ca^{2+} largely depends on the type of receptors involved in the phagocytosis process. The importance of Ca^{2+} flux from endoplasmic reticulum stores during FcγR-induced phagocytosis was clearly shown using STIM1 KO macrophages (42), and our findings are consistent with these data. Some have suggested that Ca^{2+} is not as important for phagocytosis of particles, but more important for the subsequent steps of phagosomal maturation (43). However, the data involving STIM1 KO macrophages and our data with SelK KO macrophages do not support this notion. Ingestion, signaling, and secretion of cytokines induced through FcγRs are all impaired in SelK KO macrophages. A common finding between our study with SelK KO macrophages and that involving STIM1 KO macrophages is that secretion of MCP-1 is unaffected in either case. We also found that FcγR-induced MIP-3α was not decreased in SelK KO macrophages. Thus, regulation of chemokines by Ca^{2+} may differ from pro-inflammatory cytokines, but the reasons for this are not clear. Importantly, it is possible that deletion of either SelK or STIM1 affect other cellular functions in addition to Ca^{2+} from the ER.

Overall, the data presented in this study provide important insight into the molecular mechanisms involved in producing signals and cytokines during macrophage phagocytosis of IgG-ops. particles. Particular signaling pathways (Ca^{2+} flux to ERK to nNOS) as well as subsequent effector functions rely in part on efficient Ca^{2+} flux during FcγR-induced engulfment. Some effector functions are not as dependent on SelK. For example, chemokine secretion may be less dependent on the Ca^{2+} flux in which SelK takes part than pro-inflammatory cytokines, eicosinoids, and low output NO secretion. The exact roles of SelK and Ca^{2+} during activation of macrophages and other immune cells warrant further investigation.

REFERENCES

1. Daëron, M. (1997) Fc receptor biology. *Annu. Rev. Immunol.* **15,** 203–234
2. Nimmerjahn, F., and Ravetch, J. V. (2007) Fc-receptors as regulators of immunity. *Adv. Immunol.* **96,** 179–204
3. Nimmerjahn, F., and Ravetch, J. V. (2006) Fcg receptors: old friends and new family members. *Immunity* **24,** 19–28
4. Nimmerjahn, F., Bruhns, P., Horiuchi, K., and Ravetch, J. V. (2005) FcgRIV: a novel FcR with distinct IgG subclass specificity. *Immunity* **23,** 41–51
5. Waterman, P. M., and Cambier, J. C. (2010) The conundrum of inhibitory signaling by ITAM-containing immunoreceptors: potential molecular mechanisms. *FEBS Lett.* **584,** 4878–4882
6. Mozaffarian, N., Berman, J. W., and Casadevall, A. (1995) Immune com-

plexes increase nitric oxide production by interferon-g- stimulated murine macrophage-like J774.16 cells. *J. Leukoc. Biol.* **57,** 657–662
7. Chesrown, S. E., Monnier, J., Visner, G., and Nick, H. S. (1994) Regulation of inducible nitric oxide synthase mRNA levels by LPS, INF-g, TGF-β, and IL-10 in murine macrophage cell lines and rat peritoneal macrophages. *Biochem. Biophys. Res. Commun.* **200,** 126–134
8. Paludan, S. R. (2000) Synergistic action of pro-inflammatory agents: cellular and molecular aspects. *J. Leukoc. Biol.* **67,** 18–25
9. Granger, D. L., Hibbs, J. B., Jr., Perfect, J. R., and Durack, D. T. (1988) Specific amino acid (L-arginine) requirement for the microbiostatic activity of murine macrophages. *J. Clin. Invest.* **81,** 1129–1136
10. MacMicking, J., Xie, Q. W., and Nathan, C. (1997) Nitric oxide and macrophage function. *Annu. Rev. Immunol.* **15,** 323–350
11. Tripathi, P., Kashyap, L., and Singh, V. (2007) The role of nitric oxide in inflammatory reactions. *FEMS Immunol. Med. Microbiol.* **51,** 443–452
12. Connelly, L., Jacobs, A. T., Palacios-Callender, M., Moncada, S., and Hobbs, A. J. (2003) Macrophage endothelial nitric-oxide synthase autoregulates cellular activation and pro-inflammatory protein expression. *J. Biol. Chem.* **278,** 26480–26487
13. Nathan, C. (1992) Nitric oxide as a secretory product of mammalian cells. *FASEB J.* **6,** 3051–3064
14. Kasten, T. P., Collin-Osdoby, P., Patel, N., Osdoby, P., Krukowski, M., Misko, T. P., Settle, S. L., Currie, M. G., and Nickols, G. A. (1994) Potentiation of osteoclast bone-resorption activity by inhibition of nitric oxide synthase. *Proc. Natl. Acad. Sci. U.S.A.* **91,** 3569–3573
15. Mayer, B., and Hemmens, B. (1997) Biosynthesis and action of nitric oxide in mammalian cells. *Trends Biochem. Sci.* **22,** 477–481
16. Bredt, D. S., Hwang, P. M., and Snyder, S. H. (1990) Localization of nitric oxide synthase indicating a neural role for nitric oxide. *Nature* **347,** 768–770
17. Mungrue, I. N., and Bredt, D. S. (2004) nNOS at a glance: implications for brain and brawn. *J. Cell Sci.* **117,** 2627–2629
18. Shaul, P. W. (2002) Regulation of endothelial nitric oxide synthase: location, location, location. *Annu. Rev. Physiol.* **64,** 749–774
19. Schödel, J., Padmapriya, P., Marx, A., Huang, P. L., Ertl, G., and Kuhlencordt, P. J. (2009) Expression of neuronal nitric oxide synthase splice variants in atherosclerotic plaques of apoE knockout mice. *Atherosclerosis* **206,** 383–389
20. Schmidt, H. H., Warner, T. D., Nakane, M., Förstermann, U., and Murad, F. (1992) Regulation and subcellular location of nitrogen oxide synthases in RAW264.7 macrophages. *Mol. Pharmacol.* **41,** 615–624
21. Verma, S., Hoffmann, F. W., Kumar, M., Huang, Z., Roe, K., Nguyen-Wu, E., Hashimoto, A. S., and Hoffmann, P. R. (2011) Selenoprotein K knockout mice exhibit deficient calcium flux in immune cells and impaired immune responses. *J. Immunol.* **186,** 2127–2137
22. Huang, Z., Hoffmann, F. W., Norton, R. L., Hashimoto, A. C., and Hoffmann, P. R. (2011) Selenoprotein K is a novel target of m-calpain, and cleavage is regulated by Toll-like receptor-induced calpastatin in macrophages. *J. Biol. Chem.* **286,** 34830–34838
23. Jagnandan, D., Sessa, W. C., and Fulton, D. (2005) Intracellular location regulates calcium-calmodulin-dependent activation of organelle-restricted eNOS. *Am. J. Physiol. Cell Physiol.* **289,** C1024-C1033
24. Miller, L., Alley, E. W., Murphy, W. J., Russell, S. W., and Hunt, J. S. (1996) Progesterone inhibits inducible nitric oxide synthase gene expression and nitric oxide production in murine macrophages. *J. Leukoc. Biol.* **59,** 442–450
25. Rose, D. M., Winston, B. W., Chan, E. D., Riches, D. W., Gerwins, P., Johnson, G. L., and Henson, P. M. (1997) Fc g receptor cross-linking activates p42, p38, and JNK/SAPK mitogen-activated protein kinases in murine macrophages. Role for p42MAPK in Fcγ receptor-stimulated TNF-α synthesis. *J. Immunol.* **158,** 3433–3438
26. Dong, C., Davis, R. J., and Flavell, R. A. (2002) MAP kinases in the immune response. *Annu. Rev. Immunol.* **20,** 55–72
27. Fernandez-Boyanapalli, R., McPhillips, K. A., Frasch, S. C., Janssen, W. J., Dinauer, M. C., Riches, D. W., Henson, P. M., Byrne, A., and Bratton, D. L. (2010) Impaired phagocytosis of apoptotic cells by macrophages in chronic granulomatous disease is reversed by IFN-γ in a nitric oxide-dependent manner. *J. Immunol.* **185,** 4030–4041
28. Bogdan, C. (2001) Nitric oxide and the immune response. *Nat. Immunol.* **2,** 907–916
29. Fox, S. W., and Chow, J. W. (1998) Nitric oxide synthase expression in bone cells. *Bone* **23,** 1–6
30. Schwartz, D., Mendonca, M., Schwartz, I., Xia, Y., Satriano, J., Wilson, C. B., and Blantz, R. C. (1997) Inhibition of constitutive nitric oxide synthase (NOS) by nitric oxide generated by inducible NOS after lipopolysaccharide administration provokes renal dysfunction in rats. *J. Clin. Invest.* **100,** 439–448
31. Chauhan, S. D., Seggara, G., Vo, P. A., Macallister, R. J., Hobbs, A. J., and Ahluwalia, A. (2003) Protection against lipopolysaccharide-induced endothelial dysfunction in resistance and conduit vasculature of iNOS knockout mice. *FASEB J.* **17,** 773–775
32. Nicolin, V., Ponti, C., Narducci, P., Grill, V., Bortul, R., Zweyer, M., Vaccarezza, M., and Zauli, G. (2005) Different levels of the neuronal nitric oxide synthase isoform modulate the rate of osteoclastic differentiation of TIB-71 and CRL-2278 RAW 264.7 murine cell clones. *Anat. Rec. A Discov. Mol. Cell Evol. Biol.* **286,** 945–954
33. Hecker, M., Walsh, D. T., and Vane, J. R. (1992) *J. Cardiovasc. Pharmacol.* **20,** Suppl. 12, S139-S141
34. Roman, V., Dugas, N., Abadie, A., Amirand, C., Zhao, H., Dugas, B., and Kolb, J. P. (1997) Characterization of a constitutive type III nitric oxide synthase in human U937 monocytic cells. Stimulation by soluble CD23. *Immunology* **91,** 643–648
35. Lancaster, J. R., Jr. (1997) A tutorial on the diffusibility and reactivity of free nitric oxide. *Nitric Oxide* **1,** 18–30
36. Vaughn, M. W., Kuo, L., and Liao, J. C. (1998) Estimation of nitric oxide production and reaction rates in tissue by use of a mathematical model. *Am. J. Physiol.* **274,** H2163-H2176
37. Tümer, C., Bilgin, H. M., Obay, B. D., Diken, H., Atmaca, M., and Kelle, M. (2007) Effect of nitric oxide on phagocytic activity of lipopolysaccharide-induced macrophages: possible role of exogenous L-arginine. *Cell Biol. Int.* **31,** 565–569
38. Kim, J., Park, H., Myung-Hyun, J., Han, S. H., Chung, H., Lee, J. S., Park, J. S., and Yoon, M. Y. (2008) The effects of anthrax lethal factor on the macrophage proteome: potential activity on nitric oxide synthases. *Arch. Biochem. Biophys.* **472,** 58–64
39. Young, J. D., Ko, S. S., and Cohn, Z. A. (1984) The increase in intracellular free calcium associated with IgGγ2b/γ1 Fc receptor-ligand interactions. Role in phagocytosis. *Proc. Natl. Acad. Sci. U.S.A.* **81,** 5430–5434
40. Bermelin, M., and Decker, K. (1983) Ca^{2+} flux as an initial event in phagocytosis by rat Kupffer cells. *Eur. J. Biochem.* **131,** 539–543
41. Tejle, K., Magnusson, K. E., and Rasmusson, B. (2002) Phagocytosis and phagosome maturation are regulated by calcium in J774 macrophages interacting with unopsonized prey. *Biosci. Rep.* **22,** 529–540
42. Braun, A., Gessner, J. E., Varga-Szabo, D., Syed, S. N., Konrad, S., Stegner, D., Vögtle, T., Schmidt, R. E., and Nieswandt, B. (2009) STIM1 is essential for Fcγ receptor activation and autoimmune inflammation. *Blood* **113,** 1097–1104
43. Nunes, P., and Demaurex, N. (2010) The role of calcium signaling in phagocytosis. *J. Leukoc. Biol.* **88,** 57–68